Pergamon

Bulletin of Mathematical Biology, Vol. 56, No. 4, pp. 587–616, 1994
Elsevier Science Ltd

0092-8240/94 $7.00+0.00

MODELLING THE DYNAMICS OF F-ACTIN IN THE CELL

■ GÜL CIVELEKOGLU and LEAH EDELSTEIN-KESHET
Mathematics Department,
University of British Columbia,
Vancouver, BC,
Canada V6T 1Z2

(*E.mail: gul@unixg.ubc.ca, keshet@math.ubc.ca*)

The regulation of the interactions between the actin binding proteins and the actin filaments are known to affect the cytoskeletal structure of F-actin. We develop a model depicting the formation of actin cytoskeleton, bundles and orthogonal networks, via activation or inactivation of different types of actin binding proteins. It is found that as the actin filament density increases in the cell, a spontaneous tendency to organize into bundles or networks occurs depending on the active actin binding protein concentration. Also, a minute change in the relative binding affinity of the actin binding proteins in the cell may lead to a major change in the actin cytoskeleton. Both the linear stability analysis and the numerical results indicate that the structures formed are highly sensitive to changes in the parameters, in particular to changes in the parameter ϕ, denoting the relative binding affinity and concentration of the actin binding proteins.

1. Introduction. Actin is an abundant protein in cells and an important determinant of the structure and mechanical properties of the cytoplasmic matrix. Actin polymerizes into filaments that are essential for many forms of cellular motility, including muscle contraction. In non-muscle cells, actin filaments are highly dynamic on a second to minute time scale. Since the 1970s, it has been generally recognized that in cultured cells, polymerized actin occurs in at least two distinguishable states of structural organization: in *linear fibrillar bundles*—commonly referred to as stress fibres—and in isotropic *meshworks* or networks confined to the motile lamella zones and ruffling membranes (Fig. 1a,b) (Small *et al.*, 1982; Stossel *et al.*, 1985; Stossel, 1984; Weeds, 1982).

After the discovery of the major classes of actin binding proteins in the 1980s it seemed possible that the assembly and function of actin in cells might be explained by relatively simple mechanisms involving a small handful of proteins (Cooper, 1991; Pollard and Cooper, 1986; Pollard *et al.*, 1990). Populations of actin filaments have been observed to rearrange in a variety of cells, for example during differentiation of embryonic carcinoma cells, during locomotion of fibroblasts or during development of yeast cells (see Way and Weeds, 1990; Meulemans and De Loof, 1992). It has been revealed that the

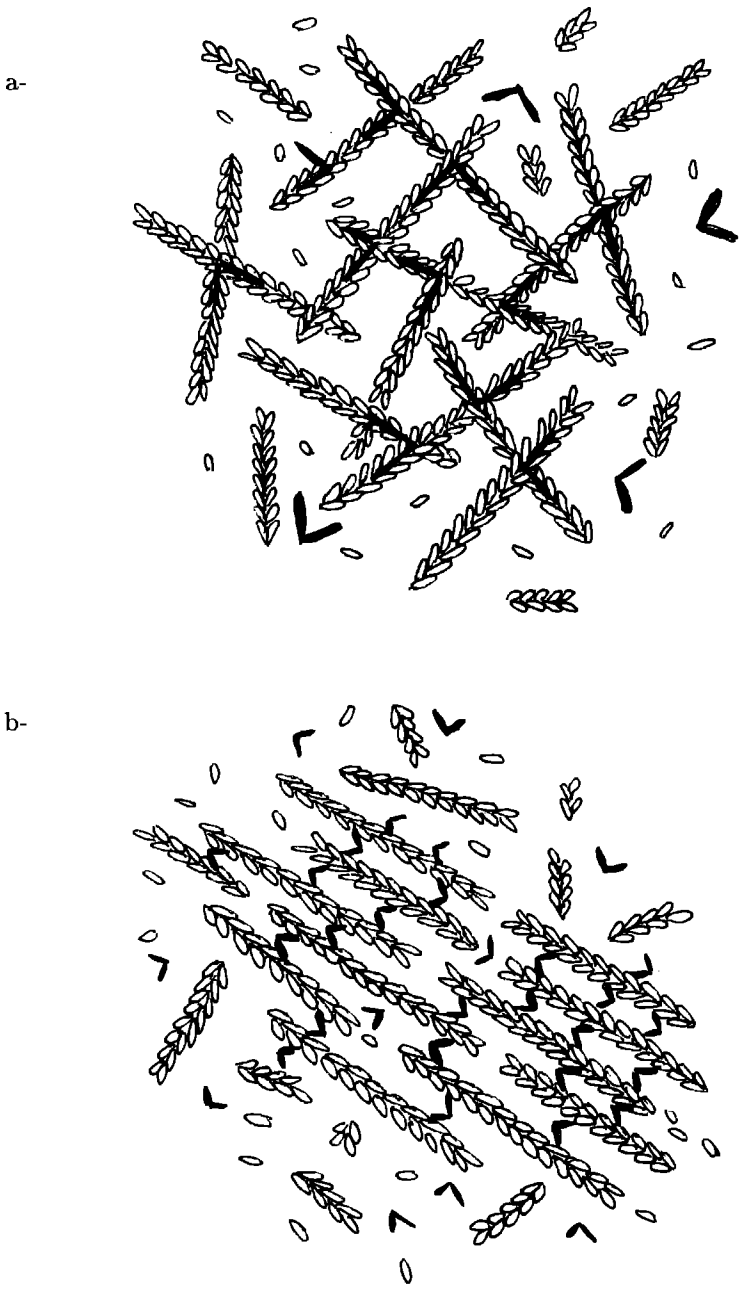

Figure 1. Network of F-actin filaments (a), joined and held nearly perpendicular by the cross-linking proteins (e.g. ABP or filamin), and bundles of F-actin filaments (b), joined and held nearly parallel by the bundling proteins (e.g. villin, fascin).

structured organization of actin filaments can also form and disappear rapidly in various cellular phenomena such as mitosis and fertilization (Pollard, 1990). The rearrangement of actin cytoskeleton in a cell is now known to affect many functions of the cell. It also plays a dominant role in various phenomena, such as the motility of bacteria in a cell. For example, the rapid movements of the bacterium *Listeria monocytogenes* through the host cell cytoplasm have been found to be mediated by the formation of a tail-like actin meshwork at the surface of the bacteria (Theriot and Mitchison, 1992; Civelekoglu and Mogilner, 1994).

A recent paper by Sherratt and Lewis (1993) develops a model of actin alignment based on mechanical response to applied forces, and to forces generated by filaments on one another. However, the rearrangement of actin cytoskeleton is also known to occur in the absence of applied forces, as a response to activation or inactivation of the binding proteins (Way and Weeds, 1990; Vandekerckhove, 1990; Korn, 1982; Hartwig, 1992; Harris, 1987). Also, the mechanical properties of the actin cytoskeleton, such as its rigidity or viscosity, have been shown to depend on the interactions between the actin binding proteins and F-actin, and specifically on the rates of reaction between them (Sato *et al.*, 1987; Stossel, 1984). In this paper we present a complementary model based on the geometry of the molecular interactions, and on the differences between binding proteins that promote a variety of actin structures that form.

The main purpose of this paper is to characterize the essential aspects of actin polymerization which permit these rapid structural changes in actin filaments. We first ask several questions about the formation of these structures. We ask which type of molecular interactions and properties observed biologically can account for the observed dynamics of actin in the cell. We also consider how properties at the molecular level (for example, affinities of binding proteins) can affect the macromolecular structure and organization, and how changes in the details of the interactions can affect the outcome of the structures that form. Towards this goal we will reformulate, in mathematical terms, the dynamics of the actin filaments in the cell based on the elements and properties reported in the biological literature (Stossel, 1990). Second, we address the question of a spontaneous switch between the orthogonal and parallel structure and the sharpness of this transition in a model that accounts for the presence of two types of actin binding proteins.

The model(s) allow us to reach the following conclusions:

(1) When the density of actin reaches a critical level, a spontaneous tendency to organize into an orthogonal or parallel structure occurs.
(2) The structure depends on the concentrations of active cross-linking or parallel binding proteins, e.g. filamin and ABP-50 or fibrillin and villin.

(3) Furthermore, the switch between the orthogonal and the parallel aligned structures can occur as a result of a change in the relative binding affinities and concentration of the two types of actin binding proteins.

The organization of this paper is as follows: in Section 2 we give some biological background and mathematical preparation for the model. In Section 3 we describe the model and discuss its analytical and numerical results. In Section 4 we extend the model to account for the existence of two types of actin binding proteins simultaneously and discuss the results of this model. Finally, we close with an overall discussion of the models and some preliminary results about the biological values of their parameters.

2. Mathematical and Biological Preparation. The steps in the formation of the actin meshwork are as follows (see Stossel, 1990; Pollard and Cooper, 1986). First, needle-like actin filaments are created by joining individual actin molecules. This process has two stages: the single molecules aggregate to form small groups of three or four molecules—*nucleation*—and then the nuclei elongate, eventually generating long, stiff rods of actin. When the length and mass of these filaments reach a certain level, the filaments start to join under the influence of cross-linking proteins in orthogonal networks or bundles. As seen under the electron microscope, some cross-linking proteins join the actin filaments at approximately right angles (Hartwig, 1992; Hartwig *et al.*, 1980, 1992; Stossel, 1984, 1990; Tilney *et al.*, 1992a,b; Weeds, 1982), whereas the bundling proteins promote binding in parallel (see Fig. 1). The way in which the cross-linking and the bundling proteins bring about the high angle branching or the parallel alignment of actin is a function of their structure (Stossel, 1984, 1990; Hartwig and Stossel, 1981; Pollard and Cooper, 1986).

The model we formulate in this paper will account for the formation of structure in a pool of actin filaments in the cell and will focus on orientation rather than spatial distributions. We assume the existence of short (ready to bind) actin filaments rather than explicitly modelling the nucleation of filaments. In the formation of the meshwork or the bundles, our focus is the orientation. An eventual goal, not addressed in this paper, is to examine a model which describes both the spatial distribution of the molecules and their orientations.

3. The Model. In this paper we consider a two-dimensional analogue of a truly three-dimensional molecular milieu. A similar simplification was made in Sherratt and Lewis (1993). The model here closely resembles a model for orientations of interacting *cells* described in Edelstein-Keshet and Ermentrout (1990). The mathematical techniques appropriate for a full three-dimensional treatment of the model are currently being developed (Mogilner and Edelstein-Keshet, 1994a,b; Civelekoglu and Mogilner, 1994).

3.1. *Definitions.* We consider only angular distributions of filaments, not spatial distributions. We distinguish between filaments which are bound to other filaments, referred to as *bound filaments*, and those which are not, referred to as *free filaments*. The model is based on the following variables:

θ = an angle, $-\pi \leqslant \theta \leqslant \pi$, with respect to some arbitrary fixed direction,
t = time,
$L(\theta, t)$ = the concentration of free actin filaments at orientation θ at time t,
$B(\theta, t)$ = the concentration of bound actin filaments at orientation θ at time t,
$K(\phi)$ = the probability that a filament contacting another filament at a relative angle ϕ binds to it in the presence of actin binding proteins,
$\rho(t)$ = the concentration of unbound binding protein at time t.

The concentrations of L and B can be described by the total length of filaments inside a unit element of the region, for example, length per unit area in a two-dimensional model, or length per unit volume in a three-dimensional version. These are analogous to the density function $F(\phi, \rho)$ defined by Sherratt and Lewis (1993), who also neglect the spatial dependence of F. Note, however, that L and B in our model are time dependent, as we explore a fully dynamic model.

The nature of the probability kernel K, discussed below, is deduced from several remarks in Stossel (1990), Hartwig and Stossel (1981), Hartwig *et al.* (1980) and Tilney *et al.* (1992a,b), taking into consideration the molecular properties and the structure of the actin binding proteins. For example, the orthogonal binding protein, ABP, promotes binding of filaments at right angles; see the histogram in Hartwig *et al.* (1980). Filament densities $L(\theta, t)$ and $B(\theta, t)$ are functions of time and of θ. Since θ is an angle of orientation, all functions of θ are assumed to be periodic, i.e. $L(-\pi, t) = L(\pi, t)$ for all t.

3.2. *Model equations.* In deriving the equations of the model we proceed from the behaviour of an individual filament. The repertoire of a single filament consists of:

(a) *rotational diffusion*, which results in tumbling and thus random reorientation of the molecules (frictional forces in the cytoplasm will limit this effect for larger molecules);
(b) *binding* upon contact with another filament and an actin binding protein (this binding is angle dependent).

Rotational diffusion, and its associated diffusion coefficient, μ, have been calculated in the literature for biopolymers (see Mossakowska *et al.*, 1988; Phillips *et al.*, 1991; Sawyer *et al.*, 1988; Thomas *et al.*, 1979).

Next, we consider how the free actin filaments binding to others can affect the free filament density at a given orientation θ, namely $L(\theta, t)$. To this end, we

first consider the likelihood that a single free filament at orientation θ attaches to another free filament, say at orientation θ', in the presence of actin binding protein. This likelihood depends on the density of free filaments oriented at θ', i.e. on $L(\theta', t)$, and on their relative orientation, i.e. on $(\theta-\theta')$. Thus, this probability will be given by:

$$\rho(t)\beta K(\theta-\theta')L(\theta', t),$$

where β is the binding affinity and $\rho(t)$ is the concentration of actin binding protein available at time t. Summing over the density of free filaments at all possible orientations results in:

$$\rho(t)\beta \int_{-\pi}^{\pi} K(\theta-\theta')L(\theta', t)\,\mathrm{d}\theta'.$$

Finally, we consider the effect of such binding on the total density of free filaments oriented at θ, which is:

$$\frac{\partial L(\theta, t)}{\partial t} = -\rho(t)\beta L(\theta, t) \int_{-\pi}^{\pi} K(\theta-\theta')L(\theta', t)\,\mathrm{d}\theta'.$$

For notational simplicity, we adopt the $*$ notation for the above convolution integral, i.e.

$$K * L = \int_{-\pi}^{\pi} K(\theta-\theta')L(\theta', t)\,\mathrm{d}\theta'.$$

As mentioned above, actin filaments bind to each other via auxiliary protein molecules of different structures. With cross-binding proteins, e.g. *ABP* or *filamin*, F-actin filaments form networks or meshworks joined at approximately 90° angles (Stossel, 1990; Tilney *et al.*, 1992a,b; Hartwig, 1992; Hartwig *et al.*, 1980; Weeds, 1982), whereas the bundling proteins, e.g. *villin* or *fascin*, produce parallel actin filaments (Cooper, 1991; Pollard and Cooper, 1986; Weeds, 1982). Therefore, we consider two types of kernel $K(\phi)$, one which accounts for orthogonal cross-linking of F-actin, and a second one accounting for the bundling of F-actin. We assume that, in the presence of a binding protein, two filaments will have some probability of binding upon contact. However, the binding probability may depend on the proper configuration being attained. In the model, the relative angle formed by the actin filaments, θ, must be within some critical range for binding to occur in each case. This is depicted by the probability $K(\theta)$. The critical range for successful binding depends on the molecular structure of the binding protein in context. The "critical angles" a and b in the equations below reflect this range for the

orthogonal binding and bundling proteins. Thus, modelling the orthogonal binding of F-actin, we consider kernels of the following form (see Fig. 2a):

$$K_1(\theta)=\begin{cases} f(\theta) & \begin{cases}|\theta+\pi/2|\leqslant a\\ |\theta-\pi/2|\leqslant a\end{cases}\\ 0 & \text{otherwise}\end{cases}$$

and, modelling parallel binding we consider the following type of kernels in turn (see Fig. 2b):

$$K_2(\theta)=\begin{cases} g(\theta) & \begin{cases}|\theta+\pi|\leqslant b\\ |\theta|\leqslant b\\ |\theta-\pi|\leqslant b\end{cases}\\ 0 & \text{otherwise}\end{cases}$$

The only assumption about $f(\theta)$ and $g(\theta)$ is that they are positive, symmetric about 0, and that f is non-increasing on $[\pi/2, \pi/2+a]$ and $[-\pi/2, -\pi/2+a]$ and g is non-increasing on $[-\pi, -\pi+b]$ and $[0, b]$ (see Fig. 2a,b). The kernels in Fig. 2 have been chosen to ease the calculations. It was argued by Edelstein-Keshet and Ermentrout (1990) that the conclusions of the model remain valid for any other function $f(\theta)$ and $g(\theta)$ satisfying the above conditions. The "critical angles" a and b, beyond which the probability of attachment is zero, represent a "range of angular attraction" ($a=20°$ and $b=30°$ in Fig. 2a and b, respectively). We also normalize K by requiring:

$$\int_{-\pi}^{\pi} K(\theta)\,\mathrm{d}\theta=1.$$

This means that the total probability, summed over all possible angles of interaction, is set to 1.

The following functional differences are assumed between L and B type filaments:

(1) free filaments reorient randomly but bound filaments do not;
(2) binding of two filaments occurs if two filaments contact in the presence of actin binding proteins;
(3) all bound filaments can become free by dissociation of proteins at some fixed unbinding rate δ;
(4) filaments can elongate by addition of actin monomers, A, at the constant rate α;
(5) filaments can shorten (lost of actin monomers from ends) at a constant rate γ.

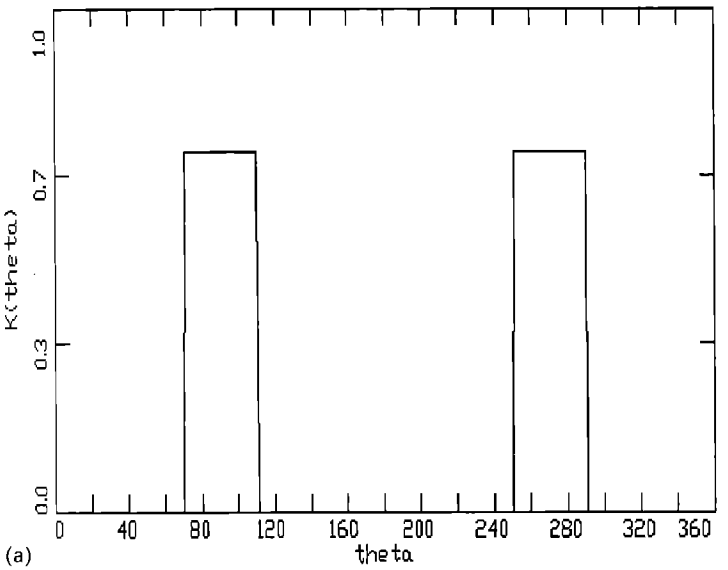

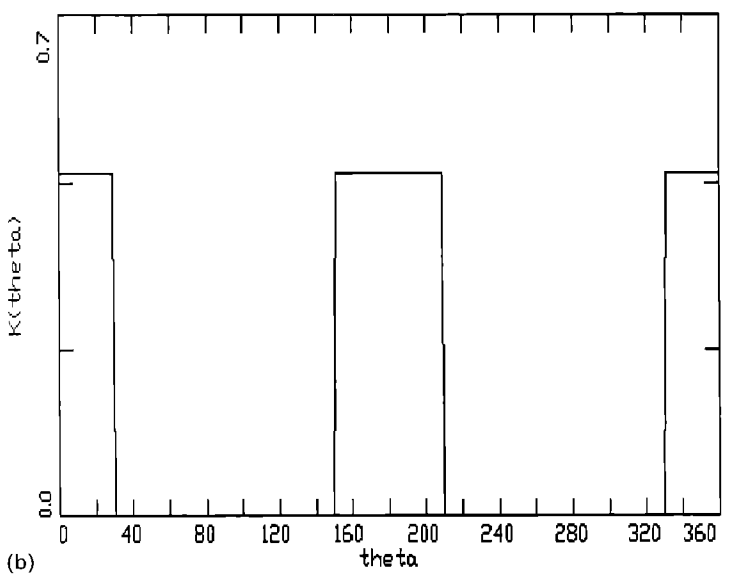

Figure 2. Shapes of angle-dependent kernels representing the probability of binding of two actin filaments via orthogonal actin binding proteins (a) and bundling proteins (b). We assume a uniform concentration of actin binding proteins in the cell. The vertical axes represent the probability function and the horizontal axes represent the angle between two contacting filaments. The "critical angles" are as follows: $a = 20°$ (a) and $b = 30°$ (b).

The following set of equations depict the interactions described above:

$$\begin{cases} \dfrac{\partial L}{\partial t}(\theta, t) = \mu \dfrac{\partial L^2}{\partial \theta^2} - \gamma L + \alpha A L + \delta B - \beta \rho L(K * B) \\ \qquad\qquad - \beta \rho L(K * L), & \text{(1a)} \\ \dfrac{\partial B}{\partial t}(\theta, t) = -\gamma B + \alpha A B - \delta B + \beta \rho B(K * L) + \beta \rho L(K * L), & \text{(1b)} \end{cases}$$

where $A(t)$ denotes the density of actin monomers at time t. The terms in equations (1) have the following meanings: $L(K * B)$ represents the rate at which the free filaments, oriented at θ, bind to bound filaments at arbitrary orientation, $L(K * L)$ denotes the rate at which they bind to free filaments at arbitrary orientation, and $B(K * L)$ denotes the rate at which free filaments oriented at arbitrary orientation bind to bound filaments oriented at θ. Also, μ denotes the rotational diffusion constant of F-actin, ρ denotes the actin binding protein concentration and β denotes the affinity of binding.

The θ-independent steady-state of these equations corresponds to the case in which the total addition of actin monomers to filaments equals the total loss of actin monomers from filaments. This equilibrium state is referred to as the *treadmilling* case in Stossel (1990). Thus, the second and the third terms in equation (1a) and the first and the second terms in equation (1b) cancel and our equations (1) reduce to equations (17) in Edelstein-Keshet and Ermentrout (1990). Also, it can be shown that the total mass density of actin filaments in the system is conserved, i.e.

$$M = \int_{-\pi}^{\pi} \{L(\theta, t) + B(\theta, t)\} \, \mathrm{d}\theta$$

is constant. The quantity M will be treated as a constant throughout the analysis. Later we will be interested in the situation in which M is allowed to vary slowly.

3.3. *Analysis.* The analysis of the model is similar to the analysis of the model in Edelstein-Keshet and Ermentrout (1990). We discuss the properties of a uniform steady-state (a time-independent state in which every orientation is equally probable) $(\bar{L}, \bar{B})$ of the system, and its stability to small perturbations of the form:

$$\begin{bmatrix} L(\theta, t) \\ B(\theta, t) \end{bmatrix} = \begin{bmatrix} \bar{L} \\ \bar{B} \end{bmatrix} + \begin{bmatrix} L_0 \\ B_0 \end{bmatrix} \mathrm{e}^{ik\theta} \mathrm{e}^{\lambda t}, \qquad (2)$$

where L_0, B_0 are small amplitudes, k is the wavenumber (the number of peaks

or the number of dominant orientations in $[0, 2\pi]$) and λ is the growth rate of the perturbation. Because θ is periodic with period 2π, the wavenumber k must be an *integer*. We seek conditions for which the perturbations are amplified with time, i.e. for which $\lambda > 0$ for some non-trivial wavenumber k.

As a result of the linear stability analysis of the full equations as in Edelstein-Keshet and Ermentrout (1990), we find that the steady-state $(\bar{L}, \bar{B})$ of (1) can be destabilized by perturbations of the form (2), provided:

$$Ck^2 < \hat{K}(1-\hat{K}), \tag{3}$$

where

$$C = \frac{\mu}{\delta}\left(\frac{\delta}{(\bar{L}+\bar{B})\beta\rho}\right)^2.$$

Here, $\hat{K}$ is the Fourier transform of the kernel K, and k is the wavenumber as above. The inequality (3) gives us a *dispersion relation*, i.e. a condition on the type of periodicity that leads to instability. Only wavenumbers satisfying (3) will give rise to *growing* structures. Thus, (3) must be satisfied for *either* bundles or networks of actin to form. We can visualize (3) graphically as done in Edelstein-Keshet and Ermentrout (1990) by plotting the right-hand side and the left-hand side of (3) on a common set of axes. This has been done in Fig. 3 for various settings of the parameters. The expression on the right-hand side of (3) as a function of k (the wavy curve in Fig. 3a,b) is fundamentally different for the two types of kernels in Fig. 2a,b and is scaled differently for different choices of "critical angles" a and b. The left-hand side of (3) is a parabola in k with coefficient C, as shown superimposed in Fig. 3a,b.

3.4. *Interpretation.* The inequality (3) depends on the shape of $\hat{K}(k)(1-\hat{K}(k))$ and on the value of C. In other words, the parabola Ck^2 must be lower than the other function at some integer value k for instability at that wavenumber. In the case where we have a kernel accounting for the orthogonal binding of F-actin, as in Fig. 2a, the first wavenumber at which the inequality (3) is satisfied is $k=4$ (see Fig. 3a). This means that a perturbation of the form $e^{4i\theta}$ grows, the steady-state loses stability and *four* orientations, 90° apart, become accentuated among all possible orientations from 0 to 2π. As a result, the filaments are mostly orthogonal to each other. In the case where we have a kernel accounting for the bundling of F-actin, as in Fig. 2b, the first such wavenumber is $k=2$, as shown in Fig. 3b. A perturbation of the form $e^{2i\theta}$ grows and results in *two* accentuated orientations 180° apart. In this case most filaments lie parallel to each other. In both cases the positions of the accentuated orientations are determined by the initial disturbance that

disrupts the steady-state. However, the spacing between them is determined by the wavenumber causing this disruption.

3.5. *Numerical methods.* The equations of the model were simulated numerically by methods described in Edelstein-Keshet and Ermentrout (1990). Numerical solutions to (1) in the case of orthogonal or parallel binding kernels

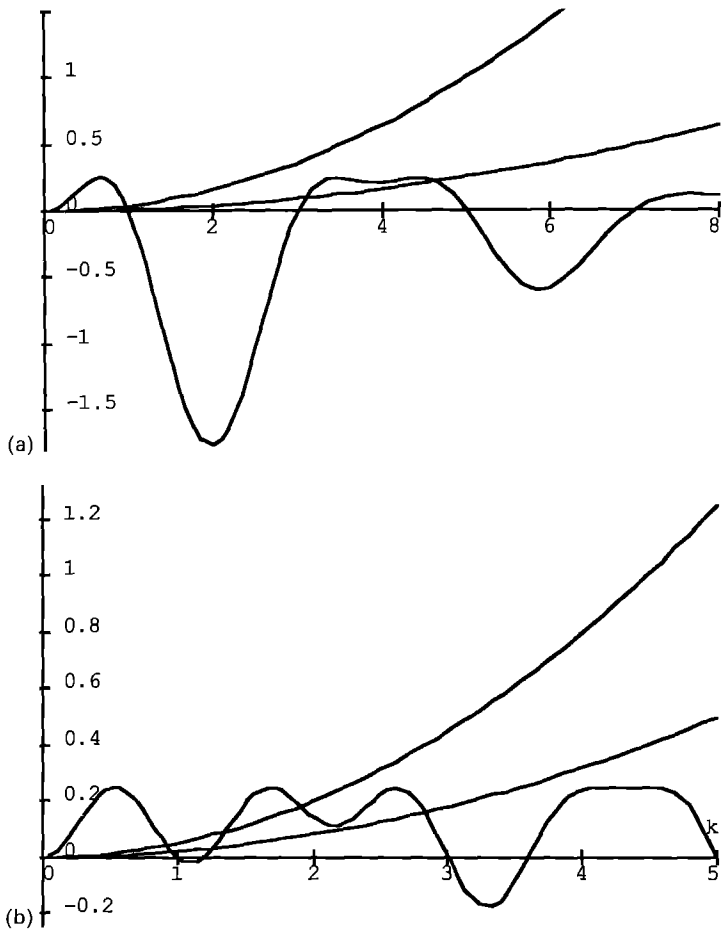

Figure 3. The expression $\hat{K}(k)(1-\hat{K}(k))$, the wavy curve in a and b, is shown as a function of the wavenumber k for $\hat{K}$, the Fourier transform of the kernels in Fig. 2a,b. Superimposed is a set of parabolas $y=Ck^2$. The uniform steady-state of (1) can be disturbed and pattern formation can be initiated only by perturbations (2), whose wavenumber k is an integer satisfying $Ck^2<\hat{K}(1-\hat{K})$, where C depends on biological parameters. The sequence of parabolas from left to right in a and b can be generated by varying the total mass of F-actin, $M=(\bar{L}+\bar{B})$, given that the other parameters are constant. Parameters are as follows: (a) the "critical angle" is $a=20°$ and the coefficient of the parabola C is 0.04 and 0.01 from left to right; (b) the "critical angle" is $b=30°$ and the coefficient of the parabola C is 0.06 and 0.02 from left to right.

are given in Figs 4a,b and 5a,b. A variety of initial densities were used, including random (in Figs 4a,b and 5a,b) or sinusoidal deviations from the steady-state or from a random homogeneous density. The magnitude of these deviations was roughly 10% of the initial homogeneous densities. The variables were discretized typically on a grid of 30–36 points ($\Delta\theta = \frac{360^\circ}{30} = 12^\circ$ and $\Delta\theta = \frac{360^\circ}{36} = 10^\circ$). We used a finite difference scheme with $\Delta t = 0.01$ and forward differencing for 15,000–100,000 iterations. The kernel in Fig. 2a was used for Fig. 4a,b and the kernel in Fig. 2b was used for Fig. 5a,b. In the results shown in Fig. 4a,b the critical angle is $a = 20^\circ$ and in Fig. 5a,b the critical angle is $b = 30^\circ$.

3.6. *Numerical results.* In Figs 4 and 5 we present the evolution of bound and free actin filament densities over time. Figure 4 shows the formation of parallel filament structures (two preferred orientations), whereas Fig. 5 shows orthogonal meshworks of filaments (four preferred orientations), as anticipated from our assumptions about the kernels in each case. It can be seen that structures that develop in the bound population are similar to those that arise in the free actin density. Pattern formation occurred either in both populations or in neither. The number of preferred orientations and their location was identical for bound and free actin filaments. However, pattern formation appeared sooner in one population than in the other for certain choices of parameters. For example, if $\delta \ll \mu$, which means biologically that the rotational diffusion of filaments is considerably higher than the dissociation rate of the actin binding proteins with filaments, pattern formation in free actin filaments took considerably longer than in the bound actin filaments. Also, in all simulations, the free actin filament density level was considerably lower than the bound actin filament density level at the final stable configuration. In the following section we will present only the evolution of the bound filament density, since the evolution of the two populations is essentially the same.

The results of the numerical simulations matched the results of the analysis and pattern formation in networks (Fig. 4a,b) or in bundles (Fig. 5a,b) was obtained for the choice of parameter values which satisfied (3). Changing any of the parameters M, μ, δ, β or ρ affects the value of the dimensionless constant C that appears in (3) and thus the stability of the system. For example, when polymerized actin starts to assemble into filaments, the total mass of actin filaments, M, increases. Therefore, C decreases and this leads to the formation of a meshwork or bundles. Similarly, increasing the binding affinity of the binding protein, β, increasing the actin binding protein concentration, ρ, or decreasing the dissociation rate of the actin binding protein, δ, in the cell result similarly in formation of meshworks or bundles.

We have also observed that, in the case where the "critical angle" a or b was either too small, a, $b \leqslant 5^\circ$, or too large, a, $b \geqslant 40^\circ$, no pattern formed (for $\approx 200{,}000$ iterations) for any choice of the other parameter values. This means

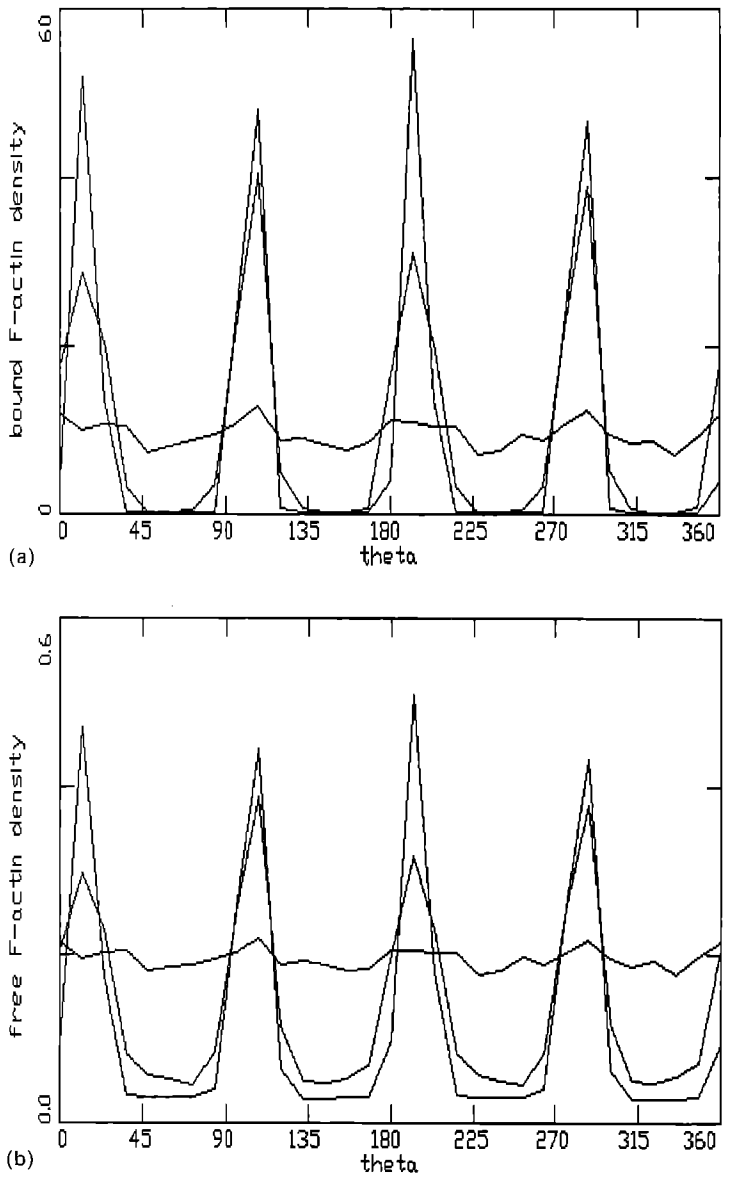

Figure 4. Formation of orthogonal network of F-actin in a pool of initially randomly distributed bound (a) and free (b) actin filaments. Numerical results for (1) are shown, where $K(\theta)$ is as in Fig. 2a. The horizontal axis is orientation and the vertical axis is the density of bound F-actin at a given orientation (a) and of free F-actin (b). Initial densities (not shown) are $L=\bar{L}+L_0(\theta, t)$, and $B=\bar{B}+B_0(\theta, t)$, where $\bar{L}=0.8$, $\bar{B}=9.2$, L_0 and B_0 are 10% random noise. Other parameters are $\delta=\beta=0.5$, $\rho=5$, $\mu=0.4$ and $M\approx 10$. The grid size is $\Delta\theta=36°$ and $\Delta t=0.01$. The solutions were found for 16,000 iterations, with plots shown at 3200, 6400 and 16,000 iterations. Note the scale on free and bound F-actin indicating that most filaments are bound. In a and b, four orientations 90° apart have been accentuated.

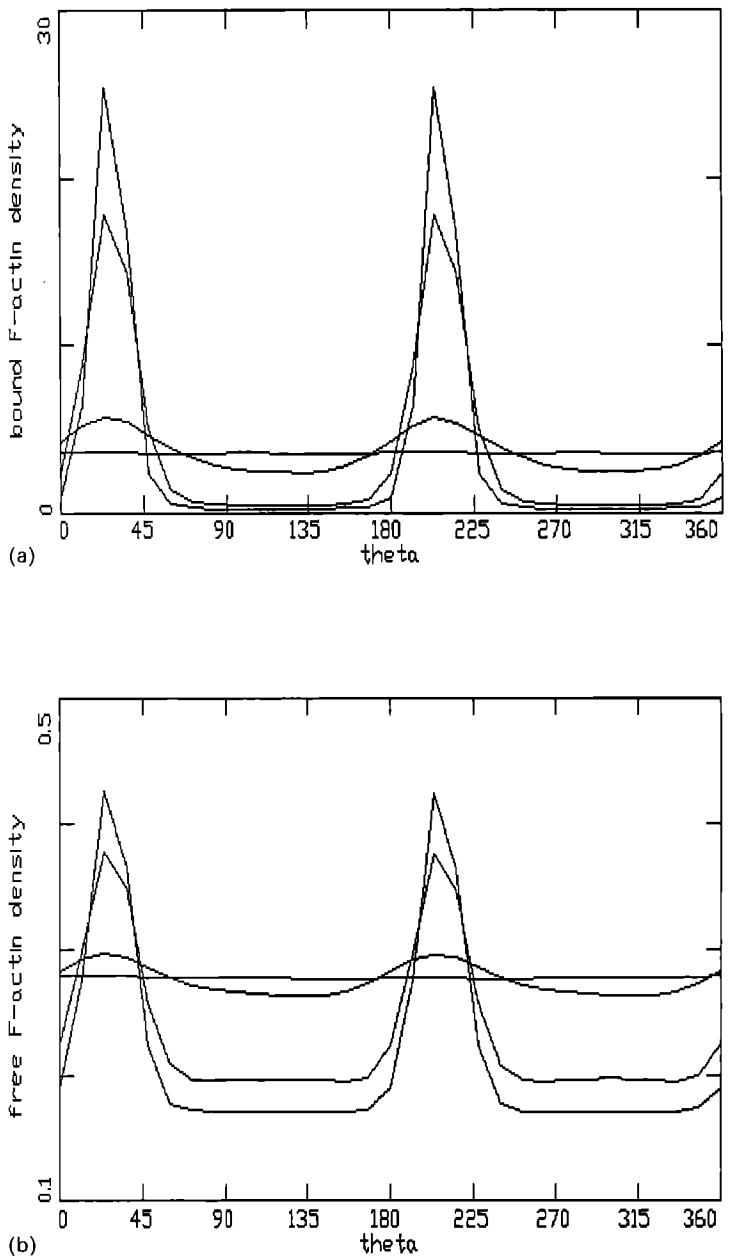

Figure 5. As in Fig. 4a,b, but showing the formation of parallel networks of F-actin. Numerical results for (1) are shown, where $K(\theta)$ is as in Fig. 2b: (a) bound actin; (b) free actin. Initial densities are as in Fig. 4, where $\bar{L}=0.5$, $\bar{B}=4.5$. Other parameters are $\delta=0.6$, $\beta=0.5$, $\rho=4$, $\mu=1.2$ and $M\approx 5$. The grid size is $\Delta\theta=10^\circ$ and $\Delta t=0.01$. The solutions were found for 30,000 iterations, with plots shown at 6000, 18,000, 24,000 and 30,000 iterations. In a and b, two orientations 180° apart have been accentuated.

that when the range of angular attraction is too small, very few filaments become bound and they are released before getting a chance to form big groups. Most filaments remain free, and thus the directional homogeneity is preserved. In the latter case, i.e. when the range of angular attraction is too wide, the filaments bind to each other at nearly every possible relative angle. Most filaments become bound with no apparent structure and, hence, the directional homogeneity is preserved in this case too.

To summarize, both numerical and analytical results of the model show that the organization of F-actin into orthogonal networks or bundles depends on the biological and chemical properties of the molecules, the parameters in the system. We will discuss the values of parameters taken from biological literature in the final section.

4. The Extended Model.

4.1. *Purpose.* In this section we consider the case where both orthogonal and parallel binding can occur. The question addressed is *under what circumstances will one of the two forms of structure dominate.* To this end we extend the model in Section 3 to account for the existence of two types of actin binding proteins simultaneously: the cross-linking and the bundling proteins. We now allow the actin filaments to bind orthogonally or in parallel depending on the ratio of the concentrations of the two types of auxiliary proteins and their binding affinities. We also investigate the transition from the network structure to the bundles and vice versa. K_1 and K_2 denote the orthogonal and the parallel binding kernels as in Section 3.2. Also ρ_1, β_1 and ρ_2, β_2 will denote the concentrations and the binding affinities of orthogonal cross-linking (1) and parallel bundling proteins (2), respectively.

4.2. *Modified equations.* The equations depicting the effect of the two types of binding simultaneously can be written as follows:

$$\begin{cases} \dfrac{\partial L}{\partial t}(\theta, t) = \mu \dfrac{\partial L^2}{\partial \theta^2} - \gamma L + \alpha A L + \delta B - \beta_1 \rho_1 L(K_1 * B) - \beta_1 \rho_1 L(K_1 * L) \\ \qquad\qquad - \beta_2 \rho_2 L(K_2 * B) - \beta_2 \rho_2 L(K_2 * L) \qquad (4a) \\ \dfrac{\partial B}{\partial t}(\theta, t) = -\gamma B + \alpha A B - \delta B + \beta_1 \rho_1 B(K_1 * L) + \beta_1 \rho_1 L(K_1 * L) \\ \qquad\qquad + \beta_2 \rho_2 B(K_2 * L) + \beta_2 \rho_2 L(K_2 * L). \qquad (4b) \end{cases}$$

In order to reduce to the previous method of analysis, we now define:

$$K = \frac{K_1 + \phi K_2}{1 + \phi}, \qquad (5)$$

where

$$\phi = \frac{\beta_2 \rho_2}{\beta_1 \rho_1} \tag{6}$$

and

$$\beta\rho = \beta_1\rho_1 + \beta_2\rho_2 = \beta_1\rho_1(1+\phi). \tag{7}$$

Here, K is a combined binding kernel and $\beta\rho$ is a combined binding affinity and binding protein density. Note that $\beta_2 = 0$ (or $\rho_2 = 0$) results in all orthogonal binding and $\beta_1 = 0$ (or $\rho_1 = 0$) results in all parallel binding, as in Section 3. For example, $\rho_2 = 0$ stands for the situation in which the parallel binding protein, villin, is absent. $\beta_2 = 0$ represents the case of binding protein that has no affinity to actin; similar conclusions hold for $\rho_1 = 0$, $\beta_1 = 0$ with respect to the orthogonal binding protein (see Table 1). The parameter ϕ represents the ratio of parallel binding to orthogonal binding, and is summarized in Table 1. For the purposes of analysis, it is convenient to vary the single parameter ϕ. As discussed later, in numerical investigations it is easier to vary β_1 and β_2. After slight rearrangement of terms, equations (4) can be reduced to the previous system, (1), but with the new kernel defined above, in (5).

In this section we study both extremes as well as intermediate situations, i.e. we are interested in all values of ϕ in $0 \leqslant \phi \leqslant \infty$. Also note that since K_1 and K_2 were normalized, so is K, and further:

$$\hat{K} = \frac{\hat{K}_1 + \phi \hat{K}_2}{1+\phi}.$$

The shape of the kernel K (see Fig. 6a,b) in this case depends not only on the two critical angles, but also on the parameter ϕ representing the ratio of the concentrations and the binding affinities of the two types of auxiliary proteins.

Table 1. The proportion of parallel and orthogonal binding can be represented by a single parameter ϕ defined by (6)

	$\phi = 0$	$\phi = 1$	$\phi = \infty$
Actin binding proteins	$\beta_2 = 0$, $\beta_1 = 1$ or $\rho_2 = 0$, $\rho_1 = 1$	$\beta_1\rho_1 = \beta_2\rho_2$	$\beta_1 = 0$, $\beta_2 = 1$ or $\rho_1 = 0$, $\rho_2 = 1$
Kernel	$K = K_1$	$K = \frac{K_1 + K_2}{2}$	$K = K_2$
Type of binding	Orthogonal binding only	Both kinds of binding occur	Parallel binding only

4.3. *Analytical results.* The analysis is identical to the previous section, and the stability condition is exactly as given in (3), but with the new interpretations of $\beta\rho$ and K as in (5) and (7). The left-hand side of (3) in this

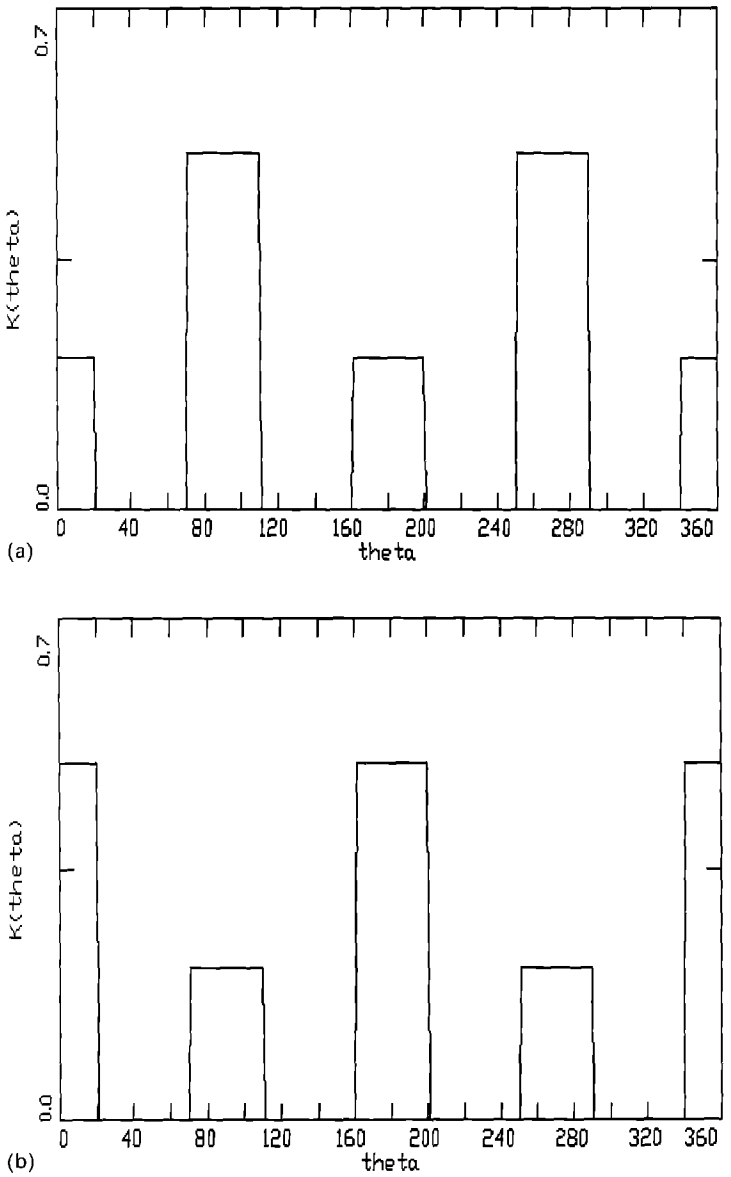

Figure 6. Shapes of the kernels K representing the combined probability of both orthogonal and parallel binding. The values of the "critical angles" are $a=20°$ for K_1 and $b=20°$ for K_2; note that K, as in (5), is also dependent on the parameter ϕ. (a) $\phi=0.43$ (for example $\beta_1=0.7$, $\beta_2=0.3$ and $\rho_1=\rho_2$). (b) $\phi=2.33$ (for example, $\beta_1=0.3$, $\beta_2=0.7$ and $\rho_1=\rho_2$).

case, too, is a parabola as a function of the wavenumber k, and its coefficient depends on the parameters in the system. The right-hand side is a function of the Fourier transform of the combined kernel, $\hat{K}$, as above.

The inequality (3) can be rearranged to obtain:

$$\frac{\mu}{\delta}\left(\frac{\delta}{(\bar{L}+\bar{B})}\right)^2 k^2 < (\beta_1\rho_1\hat{K}_1+\beta_2\rho_2\hat{K}_2)(\beta\rho-\beta_1\rho_1\hat{K}_1-\beta_2\rho_2\hat{K}_2). \tag{8}$$

In order to study the transition from the extreme case where the bundling proteins are absent, $\phi=0$, to the other extreme case where the cross-linking proteins are absent, $\phi=\infty$, we vary β_1 from 1 to 0 and β_2 from 0 to 1 simultaneously (numerically this is more convenient than letting ϕ go to ∞). The reason for this is that we wish to investigate *only* the effect of the changes of the binding affinity or binding protein ratio while *all* other conditions remain the same [see Fig. 7a–e for plots of the function on the right hand side of (8) for various values of the parameters as ϕ varies from 0 to infinity]. We also display the parabola on the left-hand side of (8) in these figures.

As in the previous section, instability at integer wavenumbers k occurs if the parabola on the left-hand side of (8) is lower than the function on the right-hand side of (8), i.e. the uniform steady-state of (4) is disrupted and pattern formation is initiated by perturbations of the form (2), whose wavenumbers satisfy (3) or equivalently (8). The first integer wavenumber for which (8) can be satisfied depends on the value of ϕ, and for the choice of critical angles $a=b=20°$, k changes from 4 to 2 as ϕ changes from zero to ∞ (or equivalently β_1 from 1 to 0 and β_2 from 0 to 1; see Fig. 7a–e). The transition from $k=4$ to $k=2$ is sharp, as predicted by the analysis, and will be discussed in the subsection below.

4.4. *Numerical results.* The numerical solutions of (4) are in agreement with the results of the analysis. The methods of the numerical computations are identical to those of the previous section. Figure 8a–e shows the numerical solutions to (4) corresponding to the kernels used in Fig. 7a–e. We note that the number of peaks that arise corresponds to the integer for which the parabolas in Fig. 7a–e *first* cross below the curve on the right-hand side of (8). For example, this occurs at $k=4$ in Fig. 7a–c, whereas at $k=2$ in Fig. 7d,e. Initial densities were random deviations from the uniform steady-state. The results of cases where deviations were sinusoidal were similar and we do not present them here.

We first summarize the results of the simulations in which the initial densities were uniform with small deviations. In the cases where the quantity ϕ was smaller than one (and even when it was equal to one in some cases), indicating a higher binding affinity or a higher concentration of the orthogonal cross-

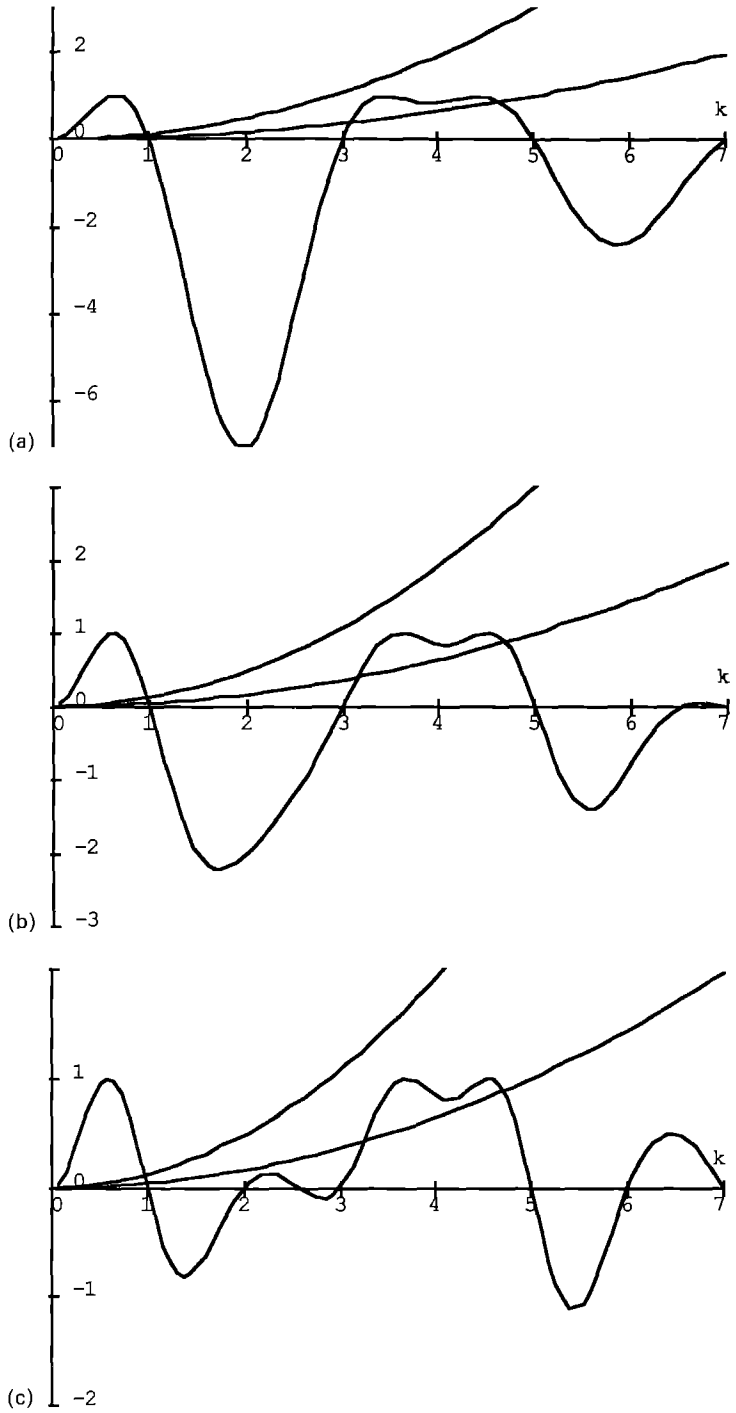

Figure 7.

linking proteins, a pattern formation in orthogonal networks resulted for the choice of parameter values which satisfied (8). For values of ϕ closer to $\phi = 1$ in some cases, first two peaks appeared and later divided into four peaks. However whether this occurs depends on the values of the "critical angles", a

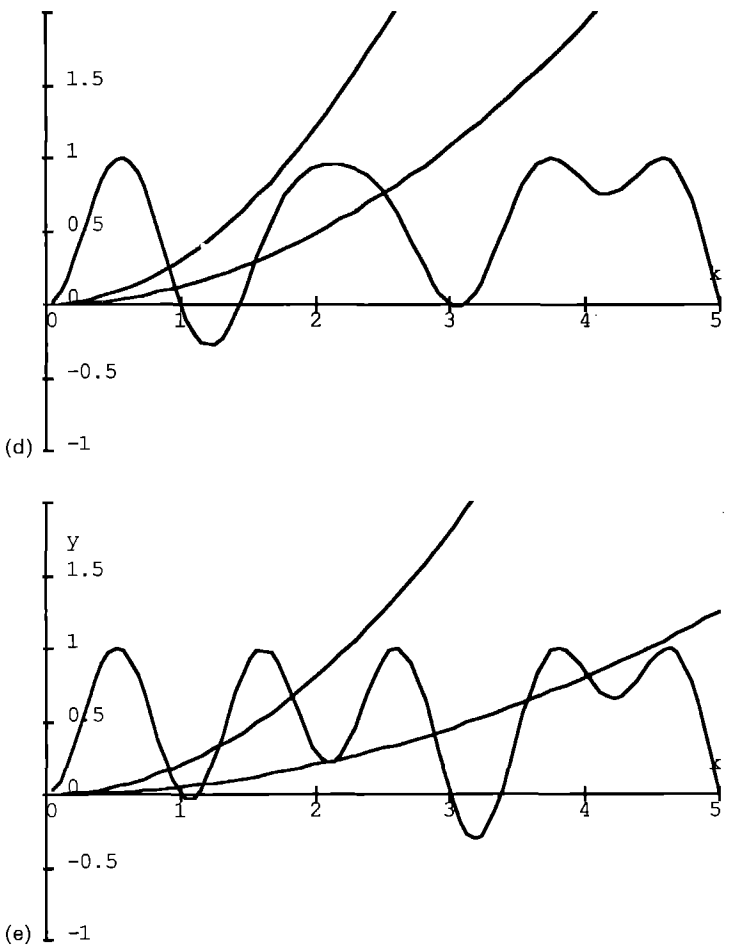

Figure 7. The expression on the right-hand side of (8) is shown as a function of the wavenumber k. K is as in Fig. 6a and b for b and d, repectively. The critical angles are $a = 20°$ for K_1 and $b = 20°$ for K_2 in all cases. Also, $\rho_1 = \rho_2 = 2$ and hence $\beta\rho = 2$ in all cases. The superimposed parabolas from left to right can be obtained by increasing the "total mass" of F-actin in the system. (a) $\beta_1 = 1$, $\beta_2 = 0$ and the coefficient C of the parabolas is 0.12 and 0.04; (b) $\beta_1 = 0.3$, $\beta_2 = 0.7$ and $C = 0.12$ and 0.04; (c) $\beta_1 = 0.5 = \beta_2$ and $C = 0.12$ and 0.04; (d) $\beta_1 = 0.7$, $\beta_2 = 0.3$ and $C = 0.3$ and 0.12; (e) $\beta_1 = 0$, $\beta_2 = 1$ and $C = 0.2$ and 0.05. The first wavenumber for which the uniform steady state is disturbed is $k = 4$ in a–c, i.e. perturbations of the form $e^{4i\theta}$ grow, resulting in four accentuated orientations 90° apart, a network structure. For d and e, the first such wavenumber is $k = 2$, i.e. perturbations of the form $e^{2i\theta}$ grow, resulting in two accentuated orientations 180° apart (bundles).

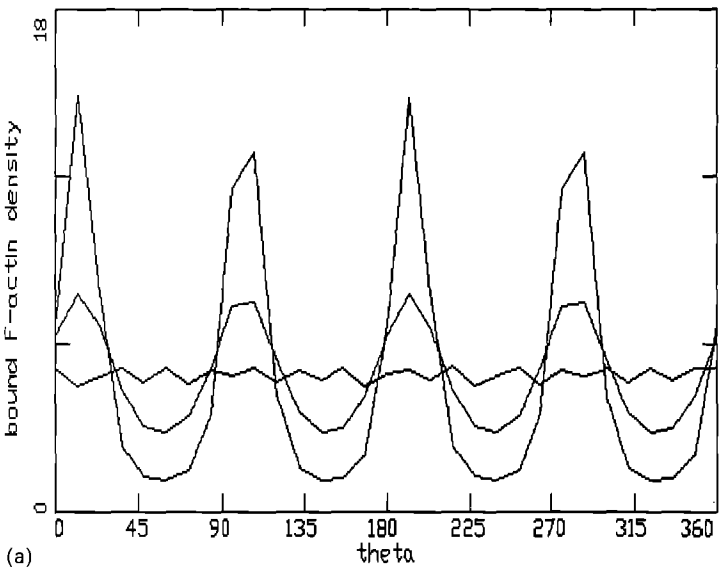
18
bound F-actin density
0
0
45
90
135
180
225
270
315
360
theta

(a)

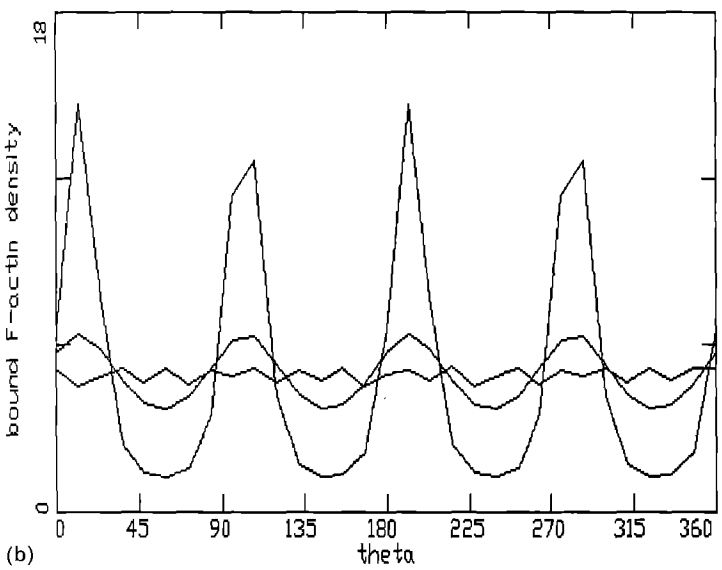
18
bound F-actin density
0
0
45
90
135
180
225
270
315
360
theta

(b)

Figure 8.

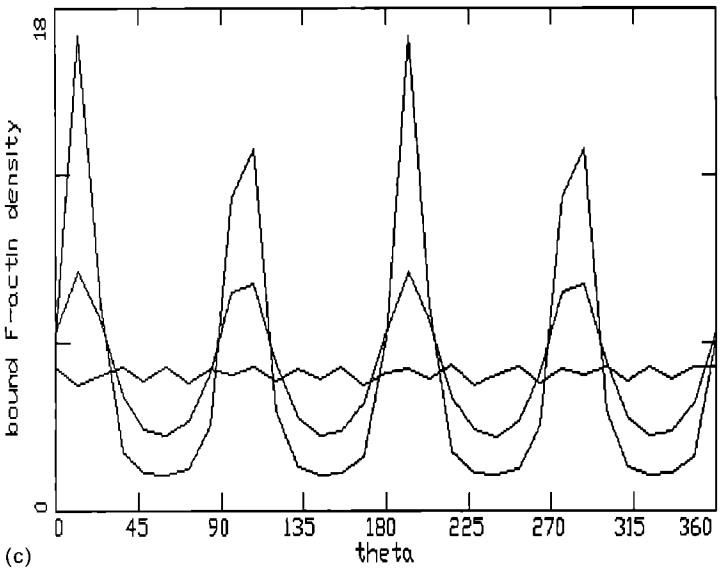
18
0
bound F-actin density
0
45
90
135
180
225
270
315
360
theta

(c)

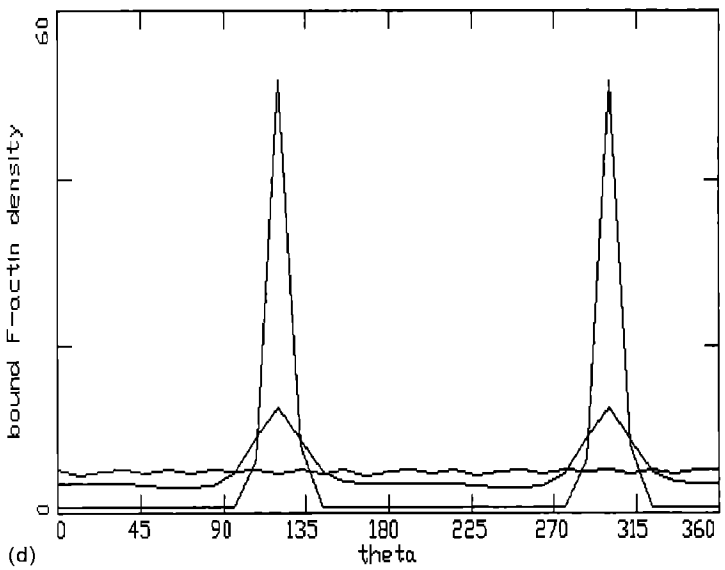
60
0
bound F-actin density
0
45
90
135
180
225
270
315
360
theta

(d)

Figure 8.

and b, and the parameter δ, which represents the dissociation rate of the binding proteins. Also, for the choice of parameter values for which $\phi = 1$, i.e. equal affinities and/or equal concentrations for both types of binding proteins, the resulting structure is dependent on the values of the "critical angles" a and b, and can be both orthogonal networks or bundles. For the values $a = 20°$ and $b = 20°$ the filaments organize into a network when $\phi = 1$ (see Fig. 8c). The transition from one type of structure to the other was very sharp, as predicted by the analysis.

We have also simulated cases with prestructured initial densities to analyse how stable these structures are to sudden changes in their environment. For example, we started with a pool of filaments organized mostly parallel to each other as in Fig. 8d, and let the parameter ϕ be very small (a sudden change from high parallel binding affinity to high orthogonal binding affinity), or we started

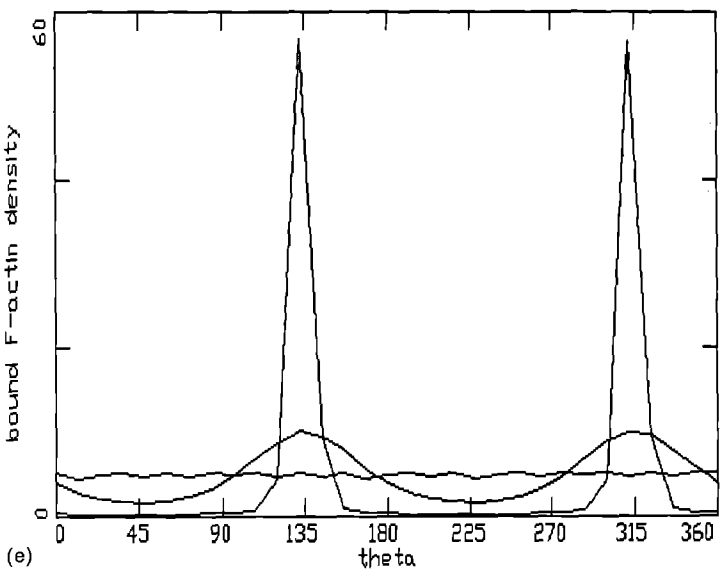

Figure 8. Formation of the network or bundles of F-actin in a pool of initially randomly distributed bound filaments and two types of binding proteins: orthogonal and parallel. $K(\theta)$ is identical to the ones used for Fig. 7a–e corresponding to a–e, respectively. Initial densities (not shown) are 10% random noise on the uniform steady-state $(\bar{L}, \bar{B})$, $\bar{L} = 0.25$ and $\bar{B} = 4.75$, and other parameters are $\beta\rho = \rho_1 = \rho_2 = 2$, $\mu = 1.84$, $\delta = 0.5$, $M \approx 5$, $\Delta t = 0.01$ and the grid size is $\Delta\theta = 12°$. The solutions were found for 70,000 iterations, with plots shown at 1, 42,000 and 70,000 iterations in a and b; 100,000 iterations, with plots shown at 1, 60,000 and 100,000 iterations in c; 50,000 iterations, with plots shown at 1, 10,000 and 50,000 iterations in d; and 130,000 iterations, with plots shown at 1, 104,000 and 130,000 iterations in e. In a–c, four orientations 90° apart have been accentuated (network structure), and in d and e two orientations 180° apart have been accentuated (bundles).

with a network of filaments as in Fig. 8b, and let the parameter ϕ be very large (a sudden change from high orthogonal binding affinity to high parallel binding affinity). Through these simulations we have found that, for the same parameter values, the same type of structure results regardless of the choice of initial densities, i.e. whether uniform or prestructured. However, in the case of prestructured initial densities the orientations that appeared were usually determined by the initial ones, with either two new peaks appearing in between the existing ones (change from bundles to networks) or two alternating peaks disappearing (change from networks to bundles). This transition does not require the complete break up of the existing structure; rather the new structure forms on the remnants of the old one. Thus, the cell is capable of switching its cytoskeletal structure, preserving its polarity, rather than choosing a random new direction after every switch. This might be compared to the situation where cells moving in a particular direction tend to continue in that direction even in the absence of external stimuli.

5. Discussion. The organization of actin filaments in the cell and its mechanical properties have been recognized to affect its shape and functions. Experimental and theoretical studies of the formation of different cytoskeletal structures and the properties of the resulting structures have been considered previously. However, in previous theoretical considerations the approach is a mechanical one, considering the effects and the balance of the forces inside and outside of the cell and neglecting the microscopic interactions and their influences on the mechanical properties of the cytogel.

Myosin is an actin binding protein which can bind to F-actin organized in networks. The actin–myosin interactions are considered to be of extreme importance in providing the cytogel its contractile behaviour. We have not, as yet, included these interactions in our model. However, we plan to extend our model to account for the actin–myosin "sliding mechanism" (Alt, 1992).

Oster *et al.* (1985) presented a model accounting for the formation of regular hexagonal patterns in microvilli solely as a consequence of the mechanical instability of the contractile acto-myosin gel. In Oster and Odell (1984), the actin–myosin meshwork is considered, and the dynamic contractile behaviour of the cytogel is captured in a model based on the mechanical properties of the gel, which in turn are regulated by a chemical trigger. In these models, the cross-links between actin filaments are assumed to be permanent, and the cytogel is viewed as an elastic material. However, according to Sato *et al.* (1987), the mechanical properties of the cytoskeleton of a cell also depend (or are influenced by) the dynamics of the rapid rearrangement of these bonds. Thus, there is a problem with the above approach, namely on the time scales of interest, the cytoskeletal network behaves as a viscous fluid with negligible

elasticity. Oster (1989) gave a review of the role of the mechanical aspects in cell motility and morphogenesis.

Other mechanical models of the contractile behaviour of the actin–myosin meshwork appear in Alt (1987) and Pohl (1990). In Alt (1987), the actin–myosin meshwork is viewed as a creeping viscous fluid with negligible elasticity. Thus, in this model the filament cross-links are not assumed to be permanent. Pohl (1990) modelled *in vitro* experiments of actin–myosin based contraction waves, stimulated by external forces, regarding the cytoplasmic matrix as a mixture of a fibroid network and an aqueous solution. Applying the laws of fluid mechanics to this mixture, he described the dynamic behaviour of the cytogel. His model is based on the Reactive Flow Model of the cytoplasm reviewed in Dembo (1989). Dembo (1989) reviewed the mechanical theory of the dynamics of the contractile cycle of the actin cytoskeleton, considering a dynamic F-actin network. In this model, the network was assumed to be isotropic and the network synthesis and breakdown, as well as the formation of cross-links between the filaments, were described by single terms in the equations.

In a recent publication, Sherratt and Lewis (1993) considered the alignment of intracellular actin filaments as a response to external forces (stress and strains) or to an anisotropy in the stress field of the filaments themselves. Their approach again is a mechanical one, based on a balance of forces in the system. Here, the interactions between the filaments, as well as the turnover rate and the strength of the bonds between them, is reflected in a single parameter: the sensitivity parameter.

The importance of the key structural elements in this phenomenon, the actin binding proteins, has been noted in the above papers. However, the interactions between the actin filaments and the binding proteins and the consequences of these interactions have not been included in any of these models.

Experimental evidence indicates that forces are not essential for the cytoskeletal rearrangement and the rapid changes in the cytoskeletal structure can be mediated by the actin binding proteins. Actin in cells can interact with several different proteins at once. The choice depends on the relative binding affinities and concentrations of different proteins and on regulatory factors (Way and Weeds, 1990). A new set of actin binding proteins may be responsible for a change in the cytoskeletal organization of a cell (Vandekerckhove, 1990). Also, the actin binding proteins may act differently under different conditions. For example, some proteins act as cross-linking proteins in the absence of Ca^{2+}, and as capping proteins in the presence of Ca^{2+}. Therefore, the sol–gel transformation can be regulated by the response of a single molecule to changes in Ca^{2+} concentrations (Korn, 1982; Hartwig, 1992). Thus, there exists biological evidence that the changes in the molecular properties of these

elements affect the resulting structure, and changes from one structure to the other also occur in the absence of external forces, via activation or inactivation of the actin binding proteins.

Based on the above evidence, we view the cell as a pool of interacting molecules. We show that the formation of different structures in the actin cytoskeleton and the switch from one structure to the other may result from the differences in the molecular properties of the elements in the cell, their interactions and their competition. To our knowledge, our model is the first one which accounts for this dynamic phenomenon. We do not imply that the mechanical viewpoint is unimportant, rather we introduce this model to complement the existing ones. We would suggest that the polymerization and self-organization of actin structures could be a first step in defining polarity and internal structure of the cell, and that mechanical forces (some of them due to the cell's environment) could then reorganize, mould or fine-tune the results.

Actin filaments are polar structures with two structurally different ends. The polarity of filaments has not yet been explicitly included in the above models but, in cases where it is important, it can readily be accommodated by a slight change. In some actin structures the filaments display locally uniform polarity, whereas in others they display opposite polarity or no polarity. The bundling proteins such as fascin, fimbrin and villin create polarized bundles (Pollard and Cooper, 1986). Unidirectionally polarized microfilament structures are found in *microvilli* of epithelial cells, and in streocilia of cochlear hair cells. Actin fibre structures which do not display any polarity are observed in the cell cortex, and in the periphery of various cells including amoebas, machrophages, leukocytes and blood platelets. in these latter cases the filaments intersect in a perpendicular fashion. In *stress fibres* in fibroblasts and in epithelial cells in culture the filaments are organized into bundles without being polarized (Stossel, 1984). The polarized binding of filaments can be accommodated in the model simply by changing the kernel, $K_2(\theta)$, in Section 3.2 to allow binding only in the case of acute contact angle. An example of this sort would be a kernel as in Fig. 2a, but without the hump in the middle. Our conclusions, and the results of the linear analysis and the numerical computations, also remain valid with this type of kernel.

Examples of actin structures considered in this paper include orthogonal networks of filaments observed in the periphery or cortical cytoplasm of motile cells, for example pseudopods, lamellipodia and membrane ruffles of moving or spreading cells and bundles of actin filaments observed in stress fibres, microvilli (column-like structures) of epithelial cells and filopodia (finger-like projections) of blood cells (Hartwig, 1980, 1992; Stossel, 1984; Way and Weeds, 1990; Weeds, 1982).

We base all interactions and physical and molecular properties on the biological data. Most of the parameters in the model appear in the biological

literature, in raw form. In Sato *et al.* (1987), the dissociation constant for the complex *Acanthamoeba* α-actinin [a cross-linking protein found in amoeba as well as in many other organisms (Pollard and Cooper, 1986; Sato *et al.*, 1987; Stossel *et al.*, 1985)] with actin filaments has been measured in sedimentation binding experiments as 26 μM. From this value, they also give estimates of the association and dissociation rate constants of the α-actinin with F-actin as 10^5–10^7 M^{-1} sec^{-1} and 2–200 sec^{-1}, respectively. These correspond to our model parameters β and γ. The values of these rate constants are known for various other actin binding proteins too (Pollard *et al.*, 1990). The rotational motion of F-actin has been studied extensively (Mossakowska *et al.*, 1988; Phillips *et al.*, 1991; Sawyer *et al.*, 1988; Thomas *et al.*, 1979). Typical values for the rotational correlation time of actin filaments of average length 1 μm is 10–100 μsec), from various cells (for example, rabbit skeletal muscle or chicken gizzard smooth muscle actin) have been measured using various techniques, for example by solid-state nuclear magnetic resonance (NMR) spectroscopy. Here, we note that these are the results of *in vitro* studies, and the average length of actin filaments *in vitro* and *in vivo* differ significantly (compare 1 and 0.1 μm). The results show that the time scale of filament motion is of the order of microseconds. The rotational diffusion coefficient, μ, of F-actin can be calculated from the rotational correlation time, viewing the actin filaments as a rigid body diffusing about its long axis. The rotational correlation time given above corresponds to a rotational diffusion coefficient of 10^3–10^4 sec^{-1}. We note that the dissociation and association rates are in comparable range with the rotational diffusion rate of F-actin. Many of the other parameters in our model, such as the elongation rate constant, δ, or the total filament concentration, M, are provided in Cooper *et al.* (1983) and Cooper (1991). Typical values are $M = 300$–400 μM (local concentration in lamellae) and $\delta = 10^7$ M^{-1} sec^{-1}. We have not yet gathered a complete set of biological parameters for our equations, but this is an important future goal. This is a rather difficult task since the parameters appearing in the literature have been measured under different circumstances (some *in vitro* and others *in vivo*), from different species and under different chemical conditions.

We finally summarize the main points and results of this paper as follows.

(1) The model presented here accounts for the dynamics of F-actin in a spatially homogeneous medium, i.e. in a well mixed cell or a specific homogeneous region in a cell. The structural differences of F-actin with respect to its spatial position are not reflected in this model.
(2) The observed dynamics of assembly and disassembly of F-actin in the cell may result simply from the interactions of the molecules in the cell, taking into consideration their physical and molecular properties. We have hypothesized that successful binding occurs only if actin filaments

are in an appropriate relative configuration (i.e. if the angles between the filaments are within a suitable range of tolerance). This is, as yet, not clearly supported by experiment, but is a reasonable assumption of the model.

(3) The switch between an orthogonal network and bundles of F-actin may result simply from a change in the binding affinities or in the concentrations of actin binding proteins (see Figs 7 and 8). These, in turn, can be governed by messages received by the cell and expression of the genes coding for these actin binding proteins.

(4) The model is presently a two-dimensional analogue of a truly three-dimensional structure. By describing the evolution of an angular distribution we are in fact investigating pattern formation on a circle. It is possible to extend this idea to three dimensions by considering pattern formation on the surface of a sphere. This is done by representing the points on the surface of a sphere by (θ, ϕ), where θ is in $[0, 2\pi]$ and ϕ is in $[0, \pi]$. The equations of the model in three dimensions are largely analogous to (1) (Mogilner and Edelstein-Keshet, 1994a,b). One studies perturbations of the uniform steady-state that are spherical harmonics, i.e. Legendre polynomials. The dispersion relation analogous to (3) or (5) then involves the inner product of K with these spherical eigenfunctions, rather than the Fourier transform $\hat{K}$. This study is currently in progress.

We would like to thank Profs W. Alt and G. F. Oster for helpful remarks and discussions, and A. Mogilner for providing preliminary results of the three-dimensional formulation of the model. This work was supported by an NSERC grant (number OGPIN 021) to Prof. L. Edelstein-Keshet and a NATO International Scientific Exchange Programmes Colaborative Research Grant (number 931073).

LITERATURE

Alt, W. 1987. Mathematical models in actin–myosin interaction. In *Fortschiritte der Zoology, Nature and Function of Cytoskeletal Proteins in Motility and Transport*, Band 34, K. E. Wohlfarth-Bottermann (Ed.), pp. 219–230. Stuttgart: Gustav Fisher Verlag.

Alt, W. 1992. Personal communication.

Civelekoglu, G. and A. Mogilner. 1994. The actin tail of *Listeria monocytogenes*. Submitted.

Cooper, J. A. 1991. The role of actin polymerization in cell motility. *Ann. Rev. Physiol.* **53**, 585–605.

Cooper, J. A., E. L. Buhle, Jr., S. B. Walker, T. Y. Tsong and T. J. Pollard. 1983. Kinetic evidence for a monomer activation step in actin polymerization. *Biochemistry* **22**, 2193–2202.

Dembo, M. 1989. Field theories of the cytoplasm. *Com. theor. Biol.* **1**(3), 159–177.

Edelstein-Keshet, L. and G. B. Ermentrout. 1990. Models for contact mediated pattern formation. *J. math. Biol.* **29**, 33–58.

Harris, H. 1987. Few answers but many questions. *Nature* **330**, 310–311.

Hartwig, J. H. 1992. Mechanisms of actin rearrangements mediating platelet activation. *J. Cell Biol.* **118**(6), 1421–1442.

Hartwig, J. H. and T. P. Stossel. 1981. Structure of macrophage actin-binding protein molecules in solution and interacting with actin filaments. *J. molec. Biol.* **145**, 563–581.

Hartwig, J. H., J. Tyler and T. P. Stossel. 1980. Actin binding protein promotes the bipolar and perpendicular branching of actin filaments. *J. Cell Biol.* **87**, 841–848.

Hartwig, J. H., M. Thelen, A. Rosen, P. A. Janmey, A. C. Nairn and A. Aderem. 1992. Marcks is an actin filament crosslinking protein regulated by protein kinease C and calcium-calmodulin. *Nature* **356**, 618–622.

Korn, E. D. 1982. Actin polymerization and its regulation by proteins from nonmuscle cells. *Physiol. Rev.* **62**(2), 672–729.

Meulemans, W. and A. De Loof. 1992. Changes in cytoskeletal actin patterns in the malphigian tubules of the fishfly, *Sarcophage bullata*, during metamorphosis. *Int. J. Insect Morphol. Embryol.* **21**(1), 1–16.

Mogilner, A. and L. Edelstein-Keshet. 1994a. Selecting a common direction: How orientational order can arise from simple contact responses between interacting cells. Submitted.

Mogilner, A. and L. Edelstein-Keshet. 1994b. Spatio-angular order in populations of self-aligning objects: formation of oriented patches. Submitted.

Mossakowska, M., J. Belagyi and H. Strzelecka-Golaszewska. 1988. An EPR study of the rotational dynamics of actins from striated and smooth muscle and their complexes with heavy meromyosin. *Eur. J. Biochem.* **175**, 557–564.

Oster, G. 1989. Cell motility and tissue morphogenesis. In *Cell Shape: Determinants, Regulation and Regulatory Role*, pp. 33–61. New York: Aademic Press.

Oster, G. F. and G. M. Odell. 1984. Mechanics of cytogels. I: oscillations in physarum. *Cell Motil.* **4**, 464–503.

Oster, G., J. D. Murray and G. M. Odell. 1985. The formation of microvilli. In *Molecular Determinants of Animal Form*, pp. 365–384. New York: Alan R. Liss.

Phillips, L., F. Seperovic, B. A. Cornell, J. A. Barden and C. G. dos Remedios. 1991. Actin dynamics studied by solid-state NMR spectroscopy. *Eur. Biophys. J.* **19**, 147–155.

Pohl, T. 1990. Periodic contraction waves in cytoplasmic extracts. In *Biological Motion: Lecture Notes in Biomathematics*, Vol. 89, W. Alt and G. Hoffmann (Eds), pp. 85–94. Berlin: Springer.

Pollard, T. D. 1990. Actin. *Curr. Opin. Cell Biol.* **2**, 33–40.

Pollard, T. D. and J. A. Cooper. 1986. Actin and actin-binding proteins. A critical evaluation of mechanisms and functions. *Ann. Rev. Biochem.* **55**, 987–1035.

Pollard, T. D., L. Satterwhite, L. Cisek, J. Corden, M. Sato and P. Maupin. 1990. Actin and myosin biochemistry in relation to cytokinesis. *Ann. N.Y. Acad. Sci.* **582**, 120–130.

Sato, M., W. H. Schwartz and T. D. Pollard. 1987. Dependence of the mechanical properties of actin/α-actinin gels on deformation rate. *Nature* **325**, 828–830.

Sawyer, W. H., A. G. Woodhouse, J. J. Csarnecki and E. Blatt. 1988. Rotational dynamics of actin. *Biochemistry* **27**, 7733–7740.

Sherratt, J. A. and J. Lewis. 1993. Stress induced alignment of actin filaments and the mechanism of cytogel. *Bull. math. Biol.* **55**, 637–654.

Small, J. V., G. Rinnerthaler and H. Hinssen. 1982. Organization of actin meshworks in cultured cells: the leading edge. *Cold Spring Harbor Symp. quant. Biol.* **46**, 599–611.

Stossel, T. P. 1984. Contribution of actin to the structure of the cytoplasmic matrix. *J. Cell Biol.* **99**(1), 15s–21s.

Stossel, T. P. 1990. How cells crawl. *Am. Sci.* **78**, 408–423.

Stossel, T. P., C. Chaponnier, R. M. Ezzel, J. H. Hartwig, P. A. Janmey *et al.* 1985. Nonmuscle actin-binding proteins. *Ann. Rev. Cell Biol.* **1**, 353–402.

Theriot, J. A. and T. J. Mitchison. 1992. The rate of actin based motility of intracellular *Listeria monocytogenes* equals the rate of actin polymerization. *Nature* **357**, 257–261.

Thomas, D. D., J. C. Seidel and J. Gergely. 1979. Rotational dynamics of spin-labeled F-actin in the sub-millisecond time range. *J. molec. Biol.* **132**, 257–273.

Tilney, L. G., D. J. DeRosier and M. S. Tilney. 1992a. How *Listeria* exploits host cell actin to form its own cytoskeleton. I. Formation of a tail and how that tail might be involved in movement. *J. Cell Biol.* **118**(1), 71–81.

Tilney, L. G., D. J. DeRosier and M. S. Tilney. 1992b. How *Listeria* exploits host cell actin to form its own cytoskeleton. II. Nucleation, actin filament polarity, filament assembly, and evidence for a pointed end capper. *J. Cell Biol.* **118**(1), 83–93.

Vandekerckhove, J. 1990. Actin-binding proteins. *Curr. Op. Cell Biol.* **2**, 41–50.

Way, M. and A. Weeds. 1990. Cytoskeletal ups and downs. *Nature* **344**, 292–294.

Weeds, A. 1982. Actin-binding proteins—regulators of cell architecture and motility. *Nature* **296**, 811–816.

Received 24 March 1993
Revised 4 October 1993